Analytical Methods

PAPER

View Article Online
View Journal | View Issue

Cite this: *Anal. Methods*, 2019, **11**, 1168

A target-induced and equipment-free biosensor for amplified visual detection of pesticide acetamiprid with high sensitivity and selectivity†

Lingwen Zeng,[a] Danhua Zhou,[b] Jinghua Wu,[a] Chengshuai Liu[c] and Junhua Chen *[b]

We have developed an equipment-free biosensor for visual pesticide residue (acetamiprid) detection with high sensitivity and selectivity. The target acetamiprid associates with an aptamer sequence and releases trigger DNA to initiate the cyclic signal amplification process. An ingeniously designed hairpin DNA probe was employed as the sensing element, which contains the same sequence as the trigger DNA in the stem part of the hairpin and a G-rich sequence in the loop part of the hairpin. An exonuclease III (Exo III)-mediated target recycling strategy was utilized to achieve quadratic amplification. This two-step cyclic signal amplification results in the generation of numerous G-quadruplex DNAzymes that can catalyze the H_2O_2-mediated oxidation of 3,3′,5,5′-tetramethylbenzidine (TMB) to generate a colored signal readout, thus providing the amplified colorimetric detection of the target. This assay is ultrasensitive, enabling the visual detection of acetamiprid at concentrations as low as 10 pM without instrumentation. Our proposed sensing system also displays high selectivity and can be applied to determine acetamiprid residues in food samples. Moreover, the assay does not involve any chemical modification of DNA, which is simple and low-cost. This sensing platform provides a promising approach for on-site detection of target molecules in resource-constrained regions because of the easy and straightforward readout of results without the use of sophisticated apparatus.

Received 19th November 2018
Accepted 25th January 2019

DOI: 10.1039/c8ay02513d

rsc.li/methods

1. Introduction

As a broad-spectrum pesticide, acetamiprid has been used globally for the treatment of agricultural pests.[1,2] It acts as the agonist of the nicotinic acetylcholine receptor, resulting in abnormal excitation, paralysis, and death of pest organisms.[3,4] The abuse of acetamiprid will lead to excessive pesticide residues in soil, water, and food products, which is a potential risk to human health.[5] Considering its serious threat, it is significant to develop an efficient and reliable analytical method for acetamiprid detection.[6–12] Conventional analytical techniques including high performance liquid chromatography (HPLC), gas chromatography (GC), liquid chromatography (LC), and mass spectrometry (MS) have been widely applied in the quantification of acetamiprid.[13,14] Although these methods are sensitive and accurate, most of them require sophisticated instruments, complex sample pretreatment, and skilled technicians, which make them unsuitable for on-site monitoring. Thus, it is urgently necessary to design an equipment-free sensing strategy for acetamiprid detection with simple operation, high sensitivity, and low cost.

Visual detection, in which the presence of the target can be observed readily by the naked eye, has attracted significant interest due to its simplicity, rapidness, and cost-effectiveness.[15–19] As the qualitative and semiquantitative results can be obtained without using any complicated and expensive instruments, visual detection is particularly important for on-site monitoring and point-of-care diagnosis.[20–25] Recently, the peroxidase-mimicking DNAzyme has been increasingly used as a colorimetric probe to construct the visual sensing platform.[26,27] For example, the G-quadruplex sequence can associate with hemin to form the peroxidase-mimicking DNAzyme which mimics the catalytic function of horseradish peroxidase.[28,29] The G-quadruplex/hemin DNAzyme can catalyze the H_2O_2-mediated oxidation of 3,3′,5,5′-tetramethylbenzidine (TMB) to the colored product $TMB^{\bullet+}$.[30,31] With the advantages of visible readout and an unmodified reporter probe, several intriguing biosensors have been developed using G-quadruplex/hemin DNAzymes as the sensing elements.[32–35] However, colorimetric assays without signal amplification often suffer from low sensitivity. Thus, visual detection of trace amounts of the target with the DNAzyme probes to harvest amplified signal output remains a major challenge.

[a]School of Food Science and Engineering, Foshan University, Foshan 528000, China
[b]Guangdong Key Laboratory of Integrated Agro-environmental Pollution Control and Management, Guangdong Institute of Eco-environmental Science & Technology, Guangzhou 510650, China. E-mail: 222chenjunhua@163.com
[c]State Key Laboratory of Environmental Geochemistry, Institute of Geochemistry, Chinese Academy of Sciences, Guiyang 550081, China

† Electronic supplementary information (ESI) available: Circular dichroism experiment, Fig. S1, and Table S1. See DOI: 10.1039/c8ay02513d

In recent years, a new class of signal amplification strategy based on nuclease (endonuclease and exonuclease)-mediated target recycling has been reported.[36] Due to the high catalytic efficiency and excellent specificity, using nuclease as the amplifier has been demonstrated to be useful in detecting trace levels of different analytes.[37] Unlike endonuclease which requires specific sequences for recognition, exonuclease does not require any specific recognition sequence, and has received more and more attention in biosensor design.[38] For example, exonuclease III (Exo III) is a kind of sequence-independent enzyme which can catalyze the stepwise removal of mononucleotides from the 3′-hydroxyl terminus of double-stranded DNA with a blunt or recessed 3′ terminus, and shows limited activity on single-stranded DNA or duplex DNA with a protruding 3′ end.[39] Thus, Exo III provides a more versatile sensing medium for amplified detection of DNA,[40] proteins,[41] metal ions,[42] and micro RNA.[43,44] To extend the new application of Exo III-assisted signal amplification, we report herein an autocatalytic DNA machine for amplified detection of pesticide acetamiprid. In the presence of the target acetamiprid, the blocked trigger DNA will be released to activate the cascade signal amplification process. An ingeniously designed hairpin probe was employed as the sensing element, which contains the same sequence as the trigger DNA in the stem part of the hairpin and a G-rich sequence in the loop part of the hairpin. Through a two-step cyclic signal amplification strategy, the hairpin probe will be converted into numerous G-quadruplex DNAzymes, which can generate an amplified colorimetric signal for acetamiprid detection. Using the G-quadruplex sequence as the visual probe, the output of the sensing system can be observed easily by the naked eye.

2. Experimental section

2.1 Chemicals and materials

Acetamiprid, TMB, hemin, dimethyl sulfoxide (DMSO), hydrogen peroxide (H_2O_2, 30 wt%), Triton X-100, ethanol, and tris-(hydroxymethyl)aminomethane (Tris) were purchased from Sigma-Aldrich (St. Louis, Mo). A hemin stock solution (5 mM) was prepared in DMSO and stored in the dark at −20 °C. Exo III was purchased from New England Biolabs (Ipswich, MA). Other reagents and chemicals were of analytical grade and used without purification. All solutions were prepared with ultrapure water (18.2 MΩ cm^{-1}) from a Millipore Milli-Q water purification system (Billerica, MA).

All DNA oligonucleotides were HPLC-purified and purchased from Shanghai Sangon Biotechnology Co., Ltd. (Shanghai, China) and their sequences were listed as follows:

Acetamiprid aptamer: 5′-TGTAATTTGTCTGCAGCGGTTCTTGATCGCT GACACCATATTATGAAGA-3′

DNA1: 5′-CAGCGATCAAGAAATATAT-3′

HP: 5′-GGGTAGGGCGGGTTGGG-CAGCGATCAAGAAATATAT- ATCGCTGCCCAACCCGCCCTACCC-TTCTTGATCGCTG-3′

(a, b, c, d mark the segments of the HP sequence)

2.2 Acetamiprid assay procedure

All DNA solutions were incubated at 95 °C for 10 min and then gradually cooled to 25 °C at a constant rate of 1 °C min^{-1}. A 150 nM aptamer was first incubated with 150 nM DNA1 in the reaction buffer (20 mM Tris–HCl, 100 mM NaCl, 10 mM $MgCl_2$, pH = 7.4) for 30 min to form a partial DNA duplex. Subsequently, different concentrations of acetamiprid were mixed with the partial DNA duplex and incubated at room temperature for 30 min. Finally, 500 nM HP and 2 units per μL Exo III were added and the mixture was incubated for 50 min at room temperature.

10 μL of hemin solution in 15 mM Tris–HCl buffer (pH 7.4, 2.5 μM hemin, 100 mM NaCl, 10 mM KCl, 10 mM $MgCl_2$, 0.01% Triton X-100, and 0.5% DMSO) was added into 40 μL of the above mixture and incubated at room temperature for 30 min. Then, 950 μL TMB–H_2O_2 substrate solution, which was constituted of 10 μL 0.5% (w/v) TMB, 20 μL 30% (w/v) H_2O_2, and 920 μL substrate buffer (containing 26.2 mM citric acid, 51.4 mM disodium hydrogen phosphate, and 25 mM KCl, pH 5.0) was added. After incubation at room temperature for 20 min, the color change of the solution was observed by the naked eye and the absorption spectrum was recorded using a UV2600 UV-vis spectrophotometer (Shimadzu).

To investigate the selectivity of the assay, other pesticides including chlorpyrifos, phoxim, dimethoate, dipterex, methyl parathion, phorate, fenthion, and isocarbophos at 100 nM were also examined by the present sensing system.

2.3 Analysis of acetamiprid in spinach leaf samples

Spinach leaves were purchased from the local market. 5 g of the spinach leaves were cut into small pieces and sprayed with acetamiprid solution. Then the leaf pieces were air-dried and extracted with 10 mL ethanol for 10 min under ultrasonic conditions. After centrifugation at 1000*g* for 10 min, the supernatant was filtered with a 0.22 μm microporous membrane and diluted 20-fold with the reaction buffer for recovery studies. The analytical procedure was the same as described above.

2.4 Native polyacrylamide gel electrophoresis (PAGE)

Different DNA solutions were incubated for 30 min at room temperature. The concentration of each oligonucleotide was 2 μM. 5 μL of each sample was mixed with 1 μL of 6× loading buffer, and then the mixture was added into the gel for electrophoresis. A 15% native polyacrylamide gel was prepared using 1× TBE buffer (89 mM Tris base, 89 mM boric acid, 2 mM EDTA, pH 8.3). PAGE was carried out in 1× TBE buffer at a constant voltage of 80 V for about 2 h at room temperature. After staining in diluted SYBR I and SYBR II solutions, the gel was scanned using a Gel Doc XR+ system (Bio-Rad).

3. Results and discussion

3.1 Design principle of the biosensor

The design principle of the target-induced and equipment-free biosensor for amplified visual detection of acetamiprid was

demonstrated in Scheme 1. A hairpin probe (HP) was ingeniously designed, which consisted of four domains. Domain a is the caged G-rich sequence. Domain b contains the same sequence as DNA1. Domain c works as a stem to stabilize the HP. Domain d is the 3′-protruding terminus. In the absence of the target acetamiprid, DNA1 was occluded by hybridization with the anti-acetamiprid aptamer, which prevented the interaction between DNA1 and domain d of the HP. Thus, this 3′ end-protruding HP is resistant to Exo III digestion, because Exo III only cleaves the blunt or recessed 3′ termini of duplex DNA. However, when acetamiprid is introduced into the sensing system, it associates with the aptamer to form acetamiprid–aptamer complexes and releases DNA1 to initiate the autocatalytic DNA machine for signal amplification. The hybridization of the liberated DNA1 with domain d of the HP would lead the HP to have a blunt 3′-terminus. Exo III then could catalyze the stepwise removal of mononucleotides from this terminus, resulting in the release of DNA1 and a secondary DNA1 analogue (the DNA fragment containing domains a and b). Both the released DNA1 and the secondary analogue can be recycled and hybridize with another hairpin probe to trigger the cyclic cleavage process. Through the two-step cyclic signal amplification on the autocatalytic DNA machine, a large number of free G-rich sequences (domain a) was generated and the detection signal can be exponentially produced. Upon incubation with hemin, the G-rich sequence can be converted into the G-quadruplex/hemin peroxidase-mimicking DNAzyme that catalyzes the H_2O_2-mediated oxidation of TMB to generate a colored signal readout, which can be easily distinguished by the naked eye. Thus, an autocatalytic signal recycling strategy for amplified visual detection of acetamiprid has been achieved.

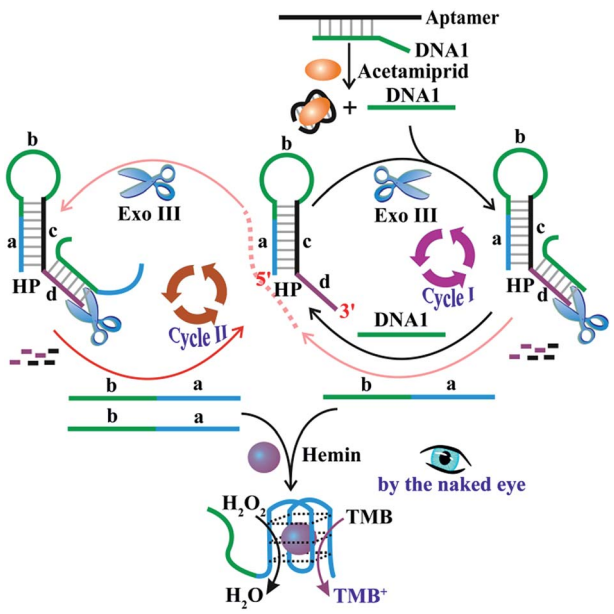

Scheme 1 Schematic illustration of the sensing principle for amplified visual detection of acetamiprid. The HP is an ingeniously designed hairpin probe containing the caged G-rich sequence (domain a). Exo III is used to carry out the cyclic cleavage process in cycles I and II.

3.2 Feasibility of the biosensing strategy

To verify the feasibility of the proposed assay strategy, the UV-vis absorption spectra and visual results of the test solution under different conditions were investigated. As shown in Fig. 1A, in the absence of acetamiprid and Exo III, only a small background absorption could be observed (curve a). With the addition of acetamiprid but no Exo III or the introduction of Exo III but no acetamiprid, the biosensor exhibited a negligible response compared with the blank test (curves b and c). In the absence of the target acetamiprid or Exo III, no cleavage reaction toward the hairpin probe could occur, and the G-rich sequence was still caged in the HP. Thus, almost no active G-quadruplex was formed. Importantly, when both acetamiprid and Exo III were present in the sensing system, we observed a dramatic increase in the absorbance intensity (curve d). This signal enhancement was attributed to the continuous cleavage process by Exo III to liberate the caged G-rich sequence in the HP. Thus, numerous active hemin/G-quadruplex DNAzymes were generated in the TMB–H_2O_2 reaction solution to give the improved colorimetric signal. The corresponding color changes of the solution (inset in Fig. 1A) were also recorded. These results clearly demonstrated that the proposed assay strategy could be used for amplified detection of acetamiprid.

The cyclic signal amplification process was further confirmed by native polyacrylamide gel electrophoresis (PAGE). As shown in Fig. 1B, the band in lane 1 corresponded to the HP.

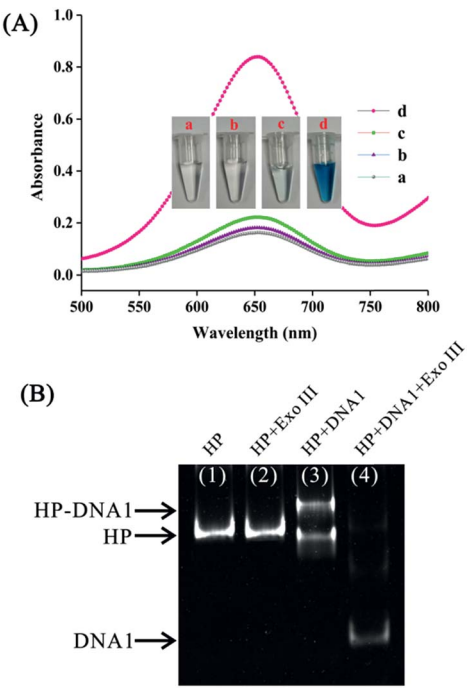

Fig. 1 (A) UV-vis absorbance spectra of the sensing system under different conditions: (a) no acetamiprid, no Exo III, (b) 10 nM acetamiprid, no Exo III, (c) no acetamiprid, 2 units per μL Exo III, and (d) 10 nM acetamiprid, 2 units per μL Exo III. Experimental results were obtained in the TMB–H_2O_2 reaction solution. Insets: the corresponding photographs of the visual results. (B) Native PAGE analysis of the Exo III-mediated signal amplification process. Concentrations for each DNA in PAGE are all 2 μM.

The HP with the 3′-protruding terminus is resistant to Exo III digestion (lane 2). When free DNA1 was present in the HP solution, the band representing the HP–DNA1 intermediate can be observed in lane 3. In the presence of Exo III, the HP–DNA1 with a blunt 3′-terminus is cleaved by Exo III, resulting in the release of DNA1, which can be recycled and hybridize with another HP to trigger the cyclic cleavage process (lane 4).

3.3 Optimization of assay conditions

To achieve the best sensing performance, the experimental conditions including the incubation temperature, the signal amplification reaction time, and the concentration of Exo III were optimized. In this assay, the incubation temperature plays an important role in the performance of the biosensor. As shown in Fig. 2A, in the presence of acetamiprid, the absorbance intensity increased with increasing incubation temperature in the range of 4–37 °C and then decreased in the range of 37–45 °C (green histogram). However, the conformation of the hairpin probe could be destroyed with increased temperature, which elevated the background signal (in the absence of acetamiprid) (blue histogram). The effect of the temperature on the conformation of the HP was also investigated by circular dichroism (Fig. S1, ESI†). In order to obtain the best signal-to-noise (S/N) ratio (red line), 25 °C was considered to be the optimum incubation temperature.

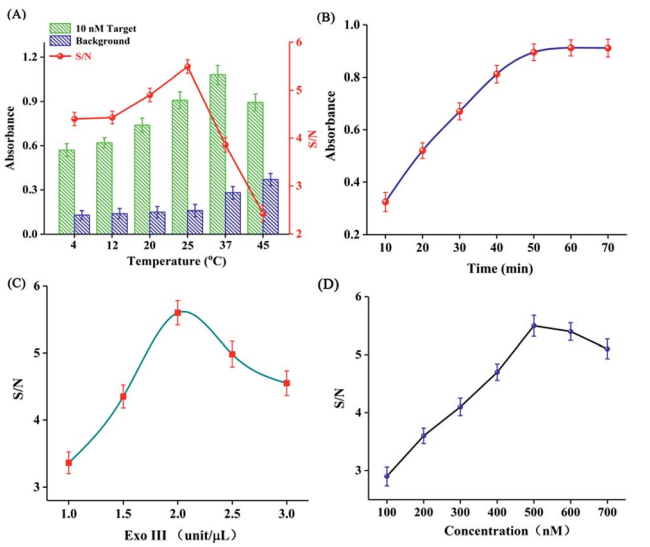

Fig. 2 (A) Effect of the incubation temperature on the performance of the biosensor. The histograms represent the absorbance intensity of the solution in the presence of 10 nM acetamiprid (green) and in the absence of acetamiprid (blue), respectively. The red line represents the S/N ratio. (B) Effect of the reaction time of signal amplification on the UV-vis absorption intensity of the proposed method for acetamiprid (10 nM) detection. Reactions were performed at room temperature. (C) Effect of the Exo III concentration on the performance of the sensing system. The acetamiprid concentration is 10 nM. Incubation temperature and reaction time were 25 °C and 50 min, respectively. (D) Effect of the HP concentration on the performance of the sensing system. The acetamiprid concentration is 10 nM. Incubation temperature, reaction time, and Exo III concentration were 25 °C, 50 min, and 2 units per μL, respectively. The error bars represent the standard deviation of three independent measurements.

As an essential factor of this assay, the reaction time is another important parameter affecting the signal amplification process of the fabricated autocatalytic sensing system. As displayed in Fig. 2B, the absorption intensity of the mixture increases rapidly with increasing reaction time in the range from 10 to 50 min and reaches a plateau thereafter, which indicated that the caged G-rich sequence was almost liberated from the HP for the colorimetric response. To ensure completion of the two-step cyclic signal amplification reactions, the reaction time of 50 min was selected for subsequent experiments.

The optical signal was also affected by the concentration of Exo III. As shown in Fig. 2C, the Exo III concentration of 2 units per μL could provide the best S/N ratio. The decreased S/N ratio at a higher amount of Exo III can be ascribed to the fact that too much enzyme would cleave the hairpin probe even in the absence of the target, resulting in a relatively high background signal. Therefore, 2 units per μL of Exo III was chosen for further investigation.

We further investigated the effect of the HP concentration on the performance of the sensing system. As shown in Fig. 2D, the S/N ratio increased with increasing the HP concentration from 100 nM to 500 nM. When the concentration was higher than 500 nM, the S/N ratio started to decrease gradually. The reason is that too much HP will cause a high background signal, while a deficient concentration of the HP will result in a weak colorimetric response. Therefore, the optimum concentration of HP was set at 500 nM.

3.4 Analytical performance for acetamiprid detection

Under the optimal experimental conditions, acetamiprid with different concentrations was added to the reaction system to investigate the detection range and sensitivity of this assay. As shown in Fig. 3A, the blue color of the solution was gradually intensified with elevated concentration of acetamiprid from 0 to 10 μM, indicating that with increasing acetamiprid concentration, more free G-quadruplexes were generated, resulting in an

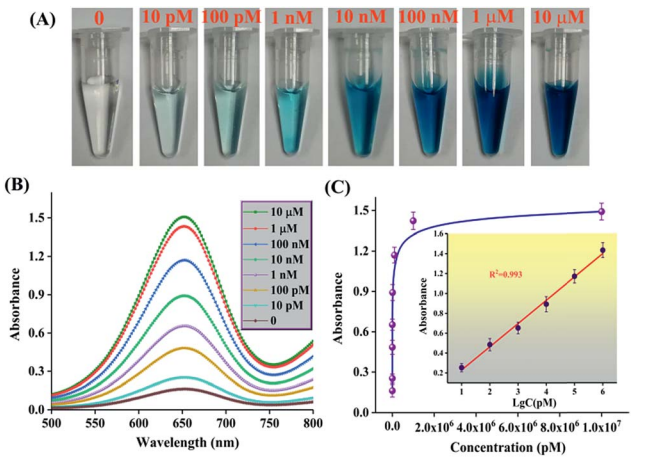

Fig. 3 (A) Photograph of visual acetamiprid detection at different concentrations. (B) Their corresponding UV-vis absorption spectra. (C) Linear relationship between the absorption intensity at 650 nm and the logarithm of AFB1 concentration. The error bars represent the standard deviation of three independent measurements.

increase in the colorimetric signal. The corresponding UV-vis absorbance spectra of the solutions were also recorded in Fig. 3B. There is a linear relationship between the absorption intensity at 650 nm and the logarithm of acetamiprid concentration in the range from 10 pM to 1 μM with a correlation coefficient (R^2) of 0.993 (Fig. 3C). The linear fitting equation is $y = 0.234x - 0.05$, where y is the absorption peak and x is the logarithm of acetamiprid concentration. Importantly, 10 pM acetamiprid can be easily identified by the naked eye according to the distinct color difference between the sample and the blank test. Such a low visual detection limit is nearly two orders of magnitude lower than that of the aptamer-based detectors for acetamiprid monitoring without signal amplification.[10,11] The quantitative limit of detection (LOD) is 2 pM. The calculated LOD is defined by $3S_0/S$, where 3 is the factor at the 99% confidence level, S_0 is the standard deviation of the blank measurements ($n = 10$), and S is the slope of the calibration curve. The sensitivity of our developed target-induced and equipment-free biosensor is comparable or even higher than that of some previously reported acetamiprid sensors (Table S1, ESI†). This high sensitivity could be attributed to the elegant design of the HP and the integrating of Exo III-assisted target recycling onto the autocatalytic DNA machine to harvest the cascade signal amplification. Most importantly, our strategy was cheap and convenient by avoiding probe modification, immobilization steps, and sophisticated signal transduction, which hold great promise for on-site detection. According to the National Food Safety Standard (China)-Maximum Residue Limits for Pesticides in Foods (GB 2763-2016), the maximum residue limit (MRL) of acetamiprid in Chinese cabbage, tomato, eggplant, and cucumber is 1 mg kg^{-1}. In this work, the linear range for acetamiprid detection is from 10 pM to 1 μM. Thus, the linear range can meet the MRL of acetamiprid. If the concentration of acetamiprid is higher than 1 μM, the sample should be diluted into the linear range before testing.

3.5 Selectivity and real sample analysis

To estimate the specificity of the proposed strategy, other pesticides including chlorpyrifos, phoxim, dimethoate, dipterex, methyl parathion, phorate, fenthion, and isocarbophos were also examined by the present sensing system. As displayed in Fig. 4, the presence of the control molecules (100 nM) causes insignificant color changes of the solutions compared with the blank sample, while the addition of the target acetamiprid (10 nM) results in a clear blue color change of the probe solution, revealing that our amplification method is highly selective. Such good specificity of the biosensor can be related to the specific aptamer–ligand interaction. In other words, only the presence of acetamiprid can trigger the amplification cycles on the autocatalytic DNA machine to achieve enhanced visual detection of the target.

Fig. 4 Selectivity tests of the visual detection method for acetamiprid against other pesticides. The concentration is 10 nM for acetamiprid and 100 nM for other control molecules.

Table 1 Analysis of real samples with acetamiprid at different concentrations

Sample	Added (nM)	Found (mean[a] ± SD[b]) (nM)	Recovery (%)
Spinach leaf 1#	0.1	0.87 ± 0.03	87
Spinach leaf 2#	1	1.04 ± 0.21	104
Spinach leaf 3#	10	10.5 ± 0.18	105
Spinach leaf 4#	50	48.2 ± 2.62	96.4
Spinach leaf 5#	100	95.8 ± 4.56	95.8

[a] Mean of three determinations. [b] SD, standard deviation.

In order to demonstrate the applicability of the acetamiprid aptasensor in practical analysis, it was employed to measure the spiked acetamiprid amounts in spinach leaf samples. The results are summarized in Table 1. Satisfactory values between 87% and 105% were obtained for the recovery experiments, which indicated that the possible interference from the complex matrix in real samples was negligible. These results suggested that the proposed assay based on the autocatalytic DNA machine could be applied to determine acetamiprid residues in food samples.

4. Conclusion

In conclusion, we have successfully developed an autocatalytic DNA machine for the visual detection of acetamiprid with cascade signal amplification on the basis of an ingeniously designed hairpin probe and Exo III. Due to the two-step cyclic signal amplification, the presence of acetamiprid results in the generation of numerous G-quadruplex/hemin DNAzymes, which cause intensified color change of the reaction solution for the highly sensitive detection of acetamiprid by the naked eye down to 10 pM. Our developed method also exhibits high selectivity toward acetamiprid against other interfering molecules. The entire assay procedure is performed under isothermal conditions and provides visual results, which minimizes the need for instrumentation, so the approach can be applied for the development of a user-friendly sensing platform for pollution monitoring in resource-limited areas. Besides, our assay protocol requires only simple mixing of label-free DNA probes to realize the signal amplification process, without the need for immobilization and wash steps, which is simple and low-cost. Significantly, the developed autocatalytic DNA machine can be extended easily to be a universal sensing platform for visual detection of other targets by simply changing the aptamer sequence. In order to reduce the reaction time and move the colorimetric biosensor much closer to field monitoring, future work will focus on developing an even faster DNA circuit with accelerated catalytic ability.

Conflicts of interest

There are no conflicts to declare.

Acknowledgements

Financial support was provided by the NSFC (31671933), the Guangdong Natural Science Funds for Distinguished Young Scholars (2016A030306012), the Local Innovative and Research Teams Project of Guangdong Pearl River Talents Program (2017BT01Z176), and the SPICC Program (2016GDASPT-0105).

References

1 W. Hu, Q. Chen, H. Li, Q. Ouyang and J. Zhao, *Biosens. Bioelectron.*, 2016, **80**, 398–404.
2 X. Liu, Y. Li, J. Liang, W. Zhu, J. Xu, R. Su, L. Yuan and C. Sun, *Talanta*, 2016, **160**, 99–105.
3 H. Li, Y. Qiao, J. Li, J. Fang, D. Fan and W. Wang, *Biosens. Bioelectron.*, 2016, **77**, 378–384.
4 R. Rapini, A. Cincinelli and G. Marrazza, *Talanta*, 2016, **161**, 15–21.
5 P. Jeschke, R. Nauen, M. Schindler and A. Elbert, *J. Agric. Food Chem.*, 2011, **59**, 2897–2908.
6 X. Yan, H. Li and X. Su, *TrAC, Trends Anal. Chem.*, 2018, **103**, 1–20.
7 P. Weerathunge, R. Ramanathan, R. Shukla, T. K. Sharma and V. Bansal, *Anal. Chem.*, 2014, **86**, 11937–11941.
8 L. Madianos, G. Tsekenis, E. Skotadis, L. Patsiouras and D. Tsoukalas, *Biosens. Bioelectron.*, 2018, **101**, 268–274.
9 D. Jiang, X. Du, L. Zhou, H. Li and K. Wang, *Anal. Chem.*, 2017, **89**, 4525–4531.
10 Y. Tian, Y. Wang, Z. Sheng, T. Li and X. Li, *Anal. Biochem.*, 2016, **513**, 87–92.
11 W. Yang, Y. Wu, H. Tao, J. Zhao, H. Chen and S. Qiu, *Anal. Methods*, 2017, **9**, 5484–5493.
12 E. Watanabe, T. Yamasaki, Y. Hirakawa, A. Harada, S. Iwasa and S. Miyake, *Anal. Methods*, 2018, **10**, 3162–3169.
13 W. Xie, C. Han, Y. Qian, H. Ding, X. Chen and J. Xi, *J. Chromatogr. A*, 2011, **1218**, 4426–4433.
14 E. Hakme, A. Lozano, C. Ferrer, F. J. Diaz-Galiano and A. R. Fernandez-Alba, *TrAC, Trends Anal. Chem.*, 2018, **100**, 167–179.
15 Z. Yang, J. Qian, X. Yang, D. Jiang, X. Du, K. Wang, H. Mao and K. Wang, *Biosens. Bioelectron.*, 2015, **65**, 39–46.
16 M. Rana, M. Balcioglu, N. M. Robertson, M. S. Hizir, S. Yumak and M. V. Yigit, *Chem. Sci.*, 2017, **8**, 1200–1208.
17 H. Shen, F. Qu, Y. Xia and X. Jiang, *Anal. Chem.*, 2018, **90**, 3697–3702.
18 S. Liu, R. Cheng, Y. Chen, H. Shi and G. Zhao, *Sens. Actuators, B*, 2018, **254**, 1157–1164.
19 M. Liu, H. Ke, C. Sun, G. Wang, Y. Wang and G. Zhao, *Talanta*, 2019, **194**, 266–272.
20 Q. Shu, L. Wang, H. Ouyang, W. Wang, F. Liu and Z. Fu, *Biosens. Bioelectron.*, 2017, **87**, 908–914.
21 M. Yang, W. Zhang, J. Yang, B. Hu, F. Cao, W. Zheng, Y. Chen and X. Jiang, *Sci. Adv.*, 2017, **3**, eaao4862.
22 Y. Xianyu, Y. Chen and X. Jiang, *Anal. Chem.*, 2015, **87**, 10688–10692.
23 R. Cheng, S. Liu, H. Shi and G. Zhao, *J. Hazard. Mater.*, 2018, **341**, 373–380.
24 J. Chang, H. Li, T. Hou and F. Li, *Biosens. Bioelectron.*, 2016, **86**, 971–977.
25 L. Han, H. Zhang, D. Chen and F. Li, *Adv. Funct. Mater.*, 2018, **28**, 1800018.
26 K. Wang, D. Fan, Y. Liu and S. Dong, *Biosens. Bioelectron.*, 2017, **87**, 116–121.
27 J. Chen, S. Zhou and J. Wen, *Angew. Chem., Int. Ed.*, 2015, **54**, 446–450.
28 T. Hou, W. Li, X. Liu and F. Li, *Anal. Chem.*, 2015, **87**, 11368–11374.
29 H. Li, J. Chang, P. Gai and F. Li, *ACS Appl. Mater. Interfaces*, 2018, **10**, 4561–4568.
30 J. Chen, J. Pan and S. Chen, *Chem. Sci.*, 2018, **9**, 300–306.
31 D. Fan, E. Wang and S. Dong, *Chem. Sci.*, 2017, **8**, 1888–1895.
32 J. Chen, S. Chen and F. Li, *Chem. Commun.*, 2017, **53**, 8743–8746.
33 Z. Shen, F. Li, Y. Jiang, C. Chen, H. Xu, C. Li, Z. Yang and Z. Wu, *Anal. Chem.*, 2018, **90**, 3335–3340.
34 W. Zhou, W. Liang, X. Li, Y. Chai, R. Ruan and Y. Xiang, *Nanoscale*, 2015, **7**, 9055–9061.
35 X. Wang, Y. Wang, X. Xiao, W. Lan, B. Zhou, S. Chen and J. Xue, *Anal. Methods*, 2018, **10**, 3081–3088.
36 X. Liu, M. Chen, T. Hou, X. Wang, S. Liu and F. Li, *Biosens. Bioelectron.*, 2014, **54**, 598–602.
37 T. Hou, X. Wang, X. Liu, T. S. Liu and F. Li, *Anal. Chem.*, 2014, **86**, 884–890.
38 L. Ge, W. Wang, X. Sun, T. Hou and F. Li, *Anal. Chem.*, 2016, **88**, 2212–2219.
39 H. Yu, J. Canoura, B. Guntupalli, O. Alkhamis and Y. Xiao, *Anal. Chem.*, 2018, **90**, 1748–1758.
40 W. Li, X. Liu, T. Hou, H. Li and F. Li, *Biosens. Bioelectron.*, 2015, **70**, 304–309.
41 L. Lu, H. Su and F. Li, *Anal. Chem.*, 2017, **89**, 8328–8334.
42 J. Chen, S. Zhou and J. Wen, *Anal. Chem.*, 2014, **86**, 3108–3114.
43 Y. Tang, M. Liu, L. Xu, J. Tian, X. Yang, Y. Zhao and S. Zhao, *Anal. Methods*, 2018, **10**, 3777–3782.
44 Q. Xu, F. Ma, S. Huang, B. Tang and C. Zhang, *Anal. Chem.*, 2017, **89**, 7077–7083.